I. SCHINDLER*[#], M. SAUER*, P. KAWULOK*, K. RODAK**, E. HADASIK**,
M. BARBARA JABŁOŃSKA**, S. RUSZ*, V. ŠEVČÁK*

STUDY OF HOT DEFORMATION BEHAVIOR OF CuFe2 ALLOY

Nil strength temperature of 1062°C and nil ductility temperature of 1040°C were experimentally set for CuFe2 alloy. The highest formability at approx. 1020°C is unusable due to massive grain coarsening. The local minimum of ductility around the temperature 910°C is probably due to minor formation of γ-iron. In the forming temperatures interval 650-950°C and strain rate 0.1-10 s^{-1} the flow stress curves were obtained and after their analysis hot deformation activation energy of 380 kJ·mol^{-1} was achieved. Peak stress and corresponding peak strain values were mathematically described with good accuracy by equations depending on Zener-Hollomon parameter.

Keywords: Copper alloy CuFe2, Hot ductility, Stress-strain curves, Hot deformation activation energy

1. Introduction

Copper and its alloys are widely used in variety of products. They show excellent electrical and thermal conductivities, good strength, formability, fatigue and high corrosion resistance. Pure copper is widely used for electrical wires and cables. Selection of such optimum conductor is always a compromise between its mechanical and electrical properties. Pure copper has high electrical conductivity, but low tensile strength; alloying increases tensile strength but decreases electrical conductivity – see e.g. [1]. Higher mechanical properties of copper alloys can be achieved by precipitation strengthening [2], strain hardening and grain refinement via cold drawing and annealing [3], or by the special methods of severe plastic deformation – high-pressure torsion [4,5], equal-channel angular pressing [6,7] or simultaneously applying rolling and transverse to the rolling direction cyclic movement of rolls [8]. Interesting possibility for controlling the structural properties of copper is also provided by processing by compression with oscillatory torsion [9] or simple torsion deformation (yielding in a gradient microstructure) [10].

The properties of copper alloys and the structure-forming processes associated with their bulk forming are in interest to many researchers, but there is relatively little information about their hot deformation behavior – under the conditions of their operational forming. The research is often realized at strain rates that are too low (e.g. 10^{-4}-10^{-3} s^{-1} for Cu-3.5%Ti alloy) [11], or simultaneously at relatively low temperatures (e.g. max. 550°C for Cu-Ti alloys) [12]. The test conditions are mostly based on specific experimental possibilities, especially for tensile tests

performed on devices such as INSTRON. Wider test conditions are achieved in compression tests on special equipment (see e.g. [13]). It is obvious why there is a lack of comprehensive data on the hot deformation behavior of copper alloys – especially in terms of their formability. The most widespread Gleeble hot deformation simulators are very difficult to be used to carry out tensile tests on copper samples because they cannot hold conventionally welded thermocouples. This is solved by fastening the thermocouple wires into drilled holes, which however negatively affects elongation to fracture. In the case of compression tests, the situation is simpler and therefore this type of hot test for copper alloys is more popular.

The aim of the experimental work was the complex investigation of the hot deformation behavior of CuFe2 precipitation-hardened copper alloy with 2.0 wt.% Fe and 0.03 wt.% P (C19400) to determine its formability and flow curves in the widest possible range of forming conditions. The results should help optimize the real processes of hot bulk forming of the examined alloy.

2. Experimental procedures

The material was prepared by melting and alloying in the open-air induction furnace. The resulting castings were approximately of dimensions Ø20 × 300 mm. On a semi-continuous laboratory rolling mill, rods Ø9.8 mm were rolled out, with a total of 6 passes using the flat oval and round grooves. The material temperatures ranged from 720 to 900°C with two inter-opera-

* VSB – TECHNICAL UNIVERSITY OF OSTRAVA, FACULTY OF METALLURGY AND MATERIALS ENGINEERING, CZECH REPUBLIC
** SILESIAN UNIVERSITY OF TECHNOLOGY, FACULTY OF MATERIALS ENGINEERING AND METALLURGY, 8 KRASIŃSKIEGO STR., 40-019 KATOWICE, POLAND

[#] Corresponding author: ivo.schindler@vsb.cz

702

tional heats applied. The rolled rods were uniformly heat treated in an electric resistance furnace with a mode 700°C/15 minutes at temperature / air.

On hot deformation simulator Gleeble 3800 a total of 4 test types were performed.

- An optical non-contact dilatometer verified the course of any significant phase transformations during resistance heating and cooling the sample Ø6 × 86 mm at rate 1°C/s (at max. temperature of 1000°C).
- Nil strength temperature (NST) was determined by a special procedure. The anisothermal test is based on the gentle tensile stress of the samples Ø6 × 81 mm by a small constant force of 80 N with the simultaneous linear increase of the temperature up to the moment of the fracture.
- The uniaxial tensile tests used samples Ø6 × 116.5 mm, resistive heated at the measured length $L_0 = 20$ mm at rate of 10° C/s directly to the deformation temperature $T = 650$-1040°C. Sample elongation to fracture took place at 100 mm/s stroke rate after delay of 180 s at deformation temperature; this corresponds to a mean strain rate of about $\dot{e} = 5$ s^{-1}. From computerized data, tensile strength [MPa] and relative elongation at break [%] related to the L_0 value were calculated.
- Heating parameters of the samples Ø8 × 12 mm for the uniaxial compression tests were similar to the tensile tests. A tantalum foil was used to reduce the friction on the flat planes of the samples (in contact with anvils). Forming temperatures of 650-950°C and strain rates of 0.1-10 s^{-1} were applied, up to a true (logarithmic) height strain of 1.0. The results of the tests were true stress – true strain curves.

3. Results and discussion

3.1. Hot plastic properties

As documented by Fig. 1, NST = 1062°C for the tested alloy. This is in line with the assumed melting point approx. 1087°C (see phase diagrams Fe-Cu published e.g. in [5, 15]).
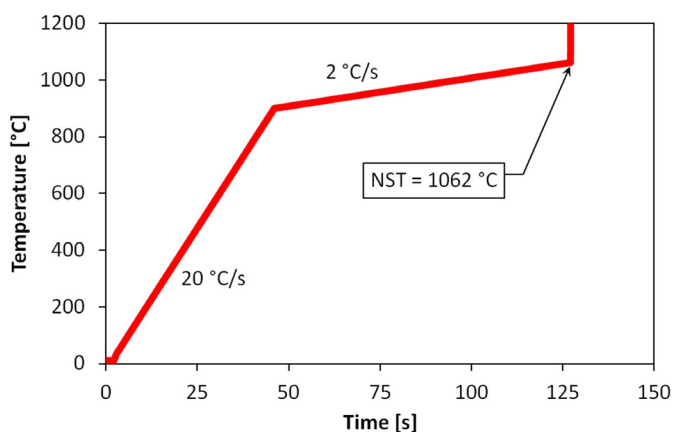

Fig. 1. The course of the test in determining NST value

In Fig. 2 the selected tensile tests are compared. Although they are burdened by scatter of the recorder signal, the highest formability of the CuFe2 alloy at surprisingly high temperature of about 1020°C is evident, and the lowest formability at the temperature of about 900°C.
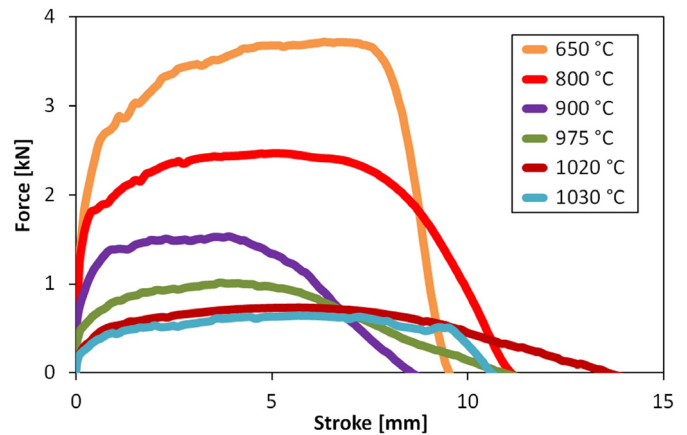

Fig. 2. Comparison of the results of selected tensile tests

This fact is better documented graphically in Fig. 3. The strength almost linearly descends to a temperature of about 975°C and then drops sharply after exceeding the temperature of 1020°C. The temperature dependence of the elongation (relative to the initial length L_0) is more complicated with a significant local minimum around the temperature of 910°C. The fall of formability at temperature above 1020°C, due to overheating and burning of the material, leads to the determination of nil ductility temperature NDT = 1040°C. This corresponds very well to the experimentally determined NST value.
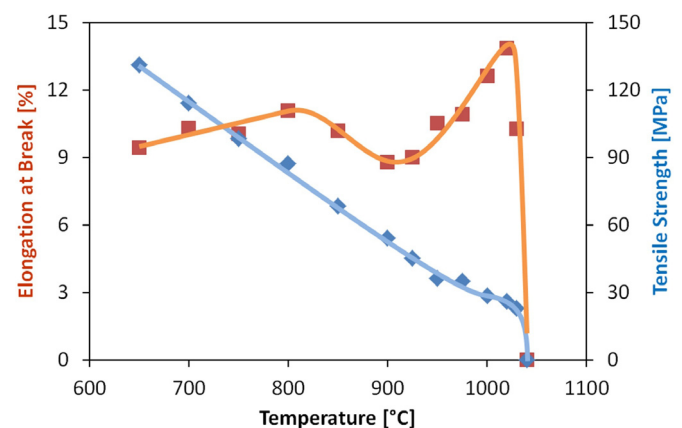

Fig. 3. Temperature dependence of ductility and tensile strength

It seems that the temperature course of the elongation was affected by the phase transformation occurring during the delay at the forming temperature (significant dynamic precipitation is not probable in the case of applied strain rates). Unfortunately, the applied optical non-contact dilatometer was not able to detect such subtle processes at relatively high heating- and cooling rate – see Fig. 4. By analyzing the Fe-Cu phase diagrams for the
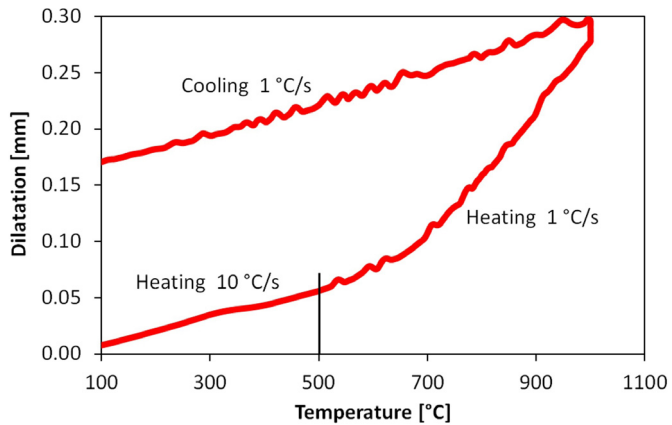
Fig. 4. Dilatometric curves during heating and cooling

Fig. 5. Fe-Cu phase diagram according to Okamoto [15]

content of 2 wt.% Fe (see e.g. [5,15-17] and Fig. 5), it can be estimated that there is pure copper (FCC phase ε) in a temperature range of about 915-1087°C. By lowering the temperature, a two-phase region with a low iron content (FCC phase γ, or BCC phase α) can be expected, i.e. $\varepsilon + \gamma$ above the temperature of about 850°C and $\varepsilon + \alpha$ at lower temperatures. This corresponds very well to the position of local maxima or minima for temperature dependance of elongation at break in Fig. 3. Particularly at low
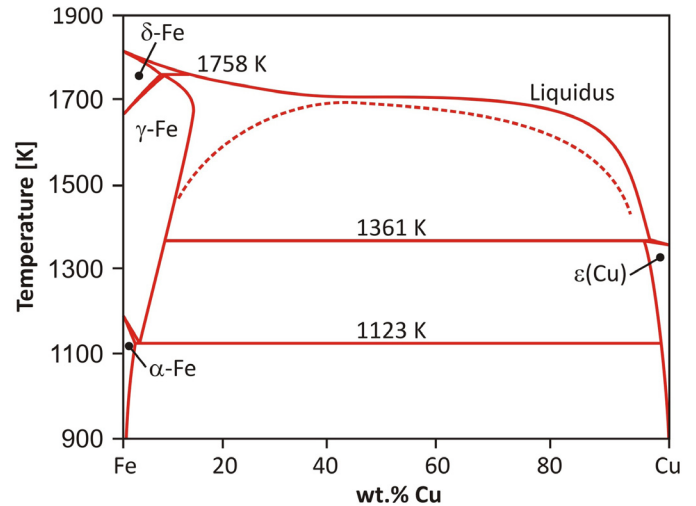
temperatures, it is imposible to exclude certain influence of the precipitating particles of Fe$_3$P on formability.

Microstructure of samples heated to 800°C, respectively 950°C was fixed by water quenching and subjected to optical metallography – see Fig. 6. Structure is composed of the fully recrystallized FCC grains of copper, in which the second phase is
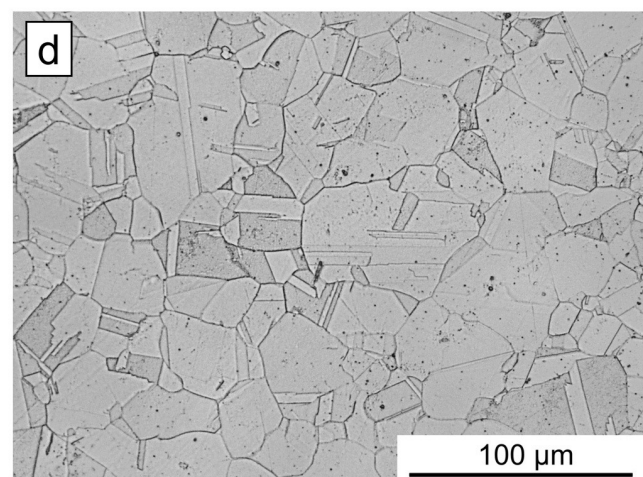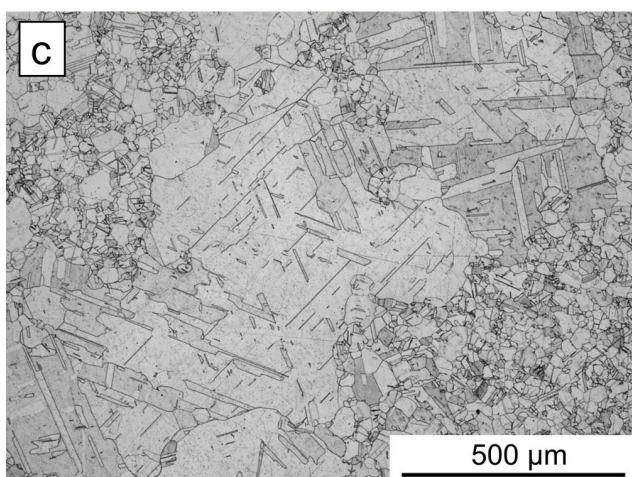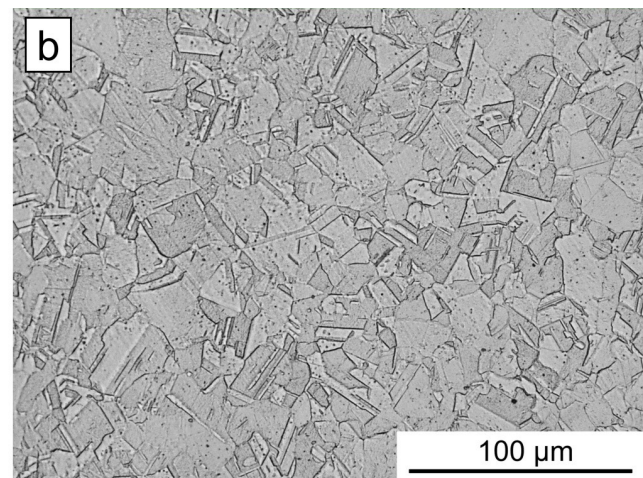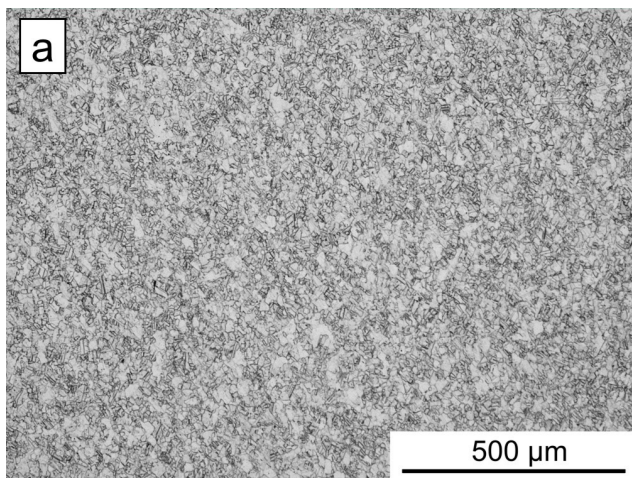

Fig. 6. Microstructure of the samples quenched from various temperature. a) temperature 800°C; b) temperature 800°C – detail; c) temperature 950°C; d) temperature 950°C – detail

formed by fine Fe particles whose dimensions are usually below 1 µm; they are well visible at higher magnification in Figs. 6b and 6d. Heating to a higher temperature resulted in a coarse grained and very inhomogeneous structure.

It should be kept in mind that the observed elongation values were influenced by holes drilled into the samples to attach the thermocouple. Thus, the values of the elongation to break cannot be understood as absolute, but only as giving the possibility to determine the trends of the temperature dependence of formability. Direct comparison with the results of other authors is also difficult for these reasons. Nagarjuna and Srinivas [12] examined the elongation of the alloy Cu-1.5Ti at a nominal strain
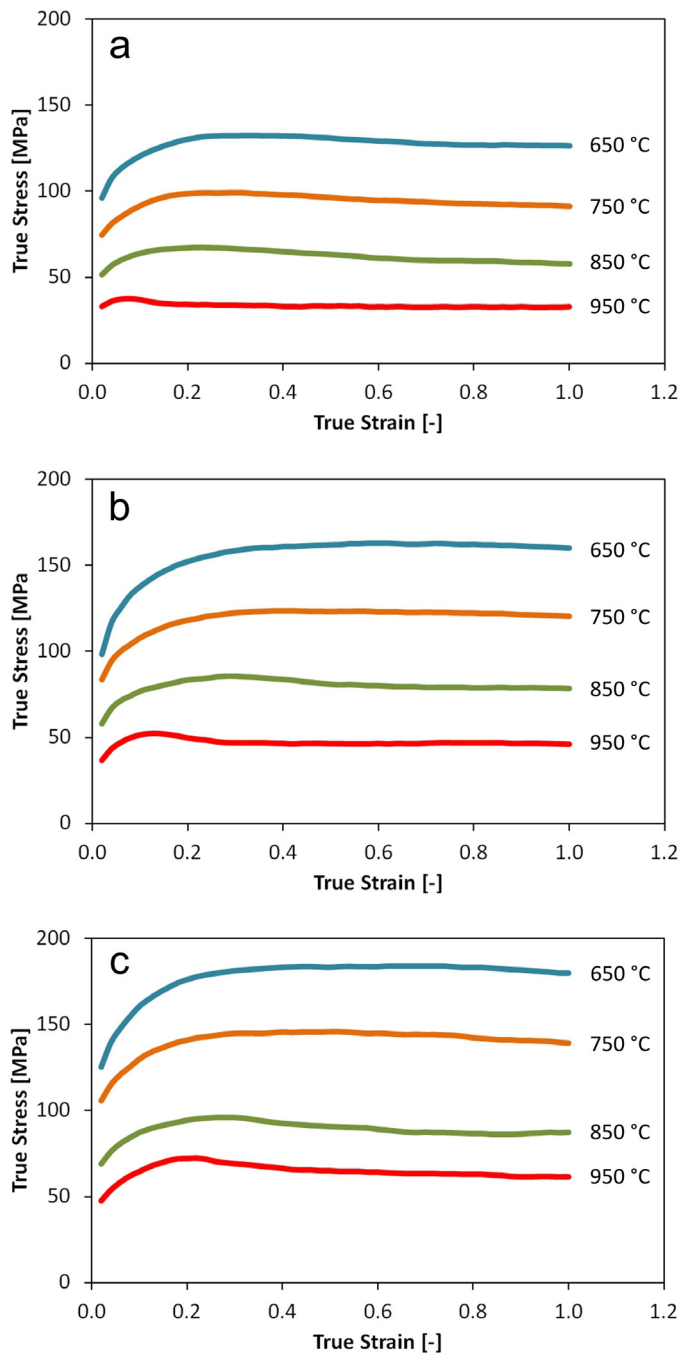
rate of 10^{-3} s^{-1} using an INSTRON universal testing system at relatively low temperatures of 250-550°C. Elongation at break of flat samples was almost constant up to 350°C (approx. 11 %) and increased with growing test temperature, to 18% at 450°C and 33% at 550°C.

3.2. Hot flow stress

In software Origin smoothed stress-strain curves are shown in Fig. 7.

For all experimentally determined curves, coordinates of stress peaks were located – strain e_p [-] and maximum (peak) stress σ_p [MPa]. Similar alloy (KFC copper with 0.13% Fe and 0.025% P) was tested by Zhang, Zhang and Peng [14]. Uniaxial compression tests were conducted at temperature of 650-850°C and strain rate of 0.01-10 s^{-1}. In comparison with CuFe2 alloy, KCF copper showcased much lower flow stress values (see Fig. 8 for example) and at low levels of strain rate even more pronounced stress drop after peak strain. Mostly did not occur even with strain of approx. 0.8 to achieve steady-state – stress-strain curves kept descending which is rather strange. Flow stress curves of the CuFe2 alloy have a much more traditional course influenced by dynamic recrystallization (primarily at temperature of 950°C).
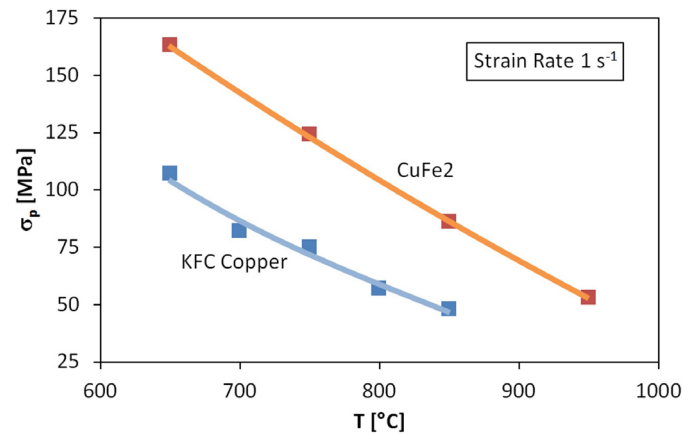

Fig. 7. Flow stress curves of the examined alloy CuFe2 in relation to temperature and strain rate. a) strain rate 0.1 s^{-1}; b) strain rate 1 s^{-1}; c) strain rate 10 s^{-1}

Fig. 8. Comparison of σ_p-values of KFC copper and CuFe2 alloy at various temperatures and one level of strain rate (coordinates of the peaks were obtained by digitization of the flow curves drawn in [14])

3.3. Hot deformation activation energy

Values of σ_p were used to calculate hot deformation activation energy Q [kJ·mol^{-1}] as described e.g. in [18] and successfully applied to various metal alloys ([19,20], etc.).

The hyperbolic law in the Arrhenius type equation is conventionally used for description of the relation between quantities σ_p, T [K] and $\dot{e}$ [s^{-1}] [21]:

$$\dot{e} = C \cdot \exp\left(\frac{-Q}{R \cdot T}\right) \cdot \left[\sinh\left(\alpha \cdot \sigma_p\right)\right]^n \qquad (1)$$

where, besides the Q-value, quantities C [s^{-1}], n [-] and α [MPa^{-1}] are material constants. Efficiency and accuracy of that constants estimate was improved by application of the specially developed interactive software ENERGY 4.0 [22]. The software uses the values n and α, determined by simple regression analyses, only as the first estimate of parameters for the final refining nonlinear regression of all the data corresponding to the Eq. (1). Such procedure ensures a higher precision of results (i.e. set of calculated constants Q, C, n and α).

This procedure has been quantified as $Q = 380$ kJ·mol^{-1} for CuFe2 alloy, which allowed for calculation of Zener-Hollomon parameter $Z(\dot{e},T)$ [s^{-1}] for given alloy. Subsequently, both coordinates of the stress peaks could be mathematically described, depending on the one defined temperature-compensated strain rate Z [23-25]:

$$\sigma_p = \frac{1}{0.025} \cdot \mathrm{arcsinh}^{4.36} \sqrt{\frac{Z}{1.01E15}} \qquad (2)$$

$$e_p = 0.003 \cdot Z^{0.11} \qquad (3)$$

$$Z = \dot{e} \cdot \exp\left(\frac{Q}{R \cdot T}\right) \qquad (4)$$

where $R = 8.314$ J·mol^{-1}·K^{-1} is the universal gas constant.

As documented in Fig. 9, the accuracy of the description of experimental data by Eq. (2) is very good over the entire range of deformation conditions; the dispersion of experimental e_p-values is always higher. Interestingly, the dependencies could always be described by one equation throughout the temperature range regardless of the effect of the changing phase composition.
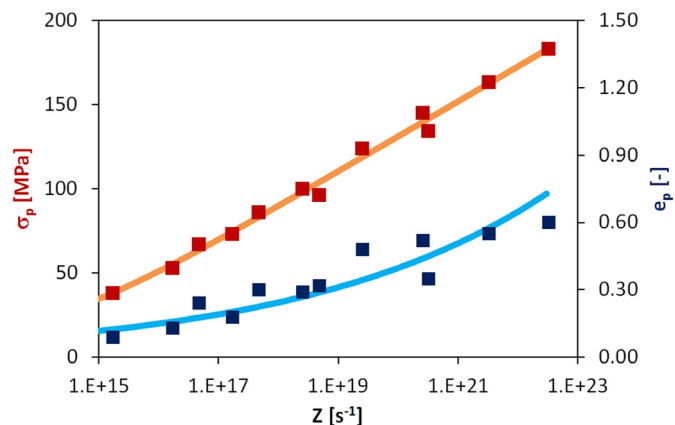

Fig. 9. Peak stress and peak strain of alloy CuFe2 as a function of Zener-Hollomon parameter

Using the same methodology (applying the final non-linear regression in ENERGY software) the value of $Q = 284$ kJ·mol^{-1} for KFC copper was obtained; this is very close to 289 kJ·mol^{-1} obtained in the course of work [14]. It is obvious that the different chemical composition of the CuFe2 alloy not only led to a significant increase in the deformation resistance (see Fig. 6) but also to a Q-value increase of one third. According to [26], hot

deformation activation energy of 389 kJ·mol^{-1} was calculated in temperature range of 700-900°C for Cu-3.45% Ti alloy which is practically the same value as that obtained for the CuFe2 alloy. Gao et al. [13] studied the hot deformation behavior of copper with different purities. The samples were compressed at temperatures of 250-500°C under various strain rates of 10^{-4}-10^{-1} s^{-1}. The Q-value was affected by materials purity, i.e. about 210 kJ·mol^{-1} for purities 6N or 7N, and 245 kJ·mol^{-1} for purity 4N of copper.

4. Conclusions

- Using the experimental potential of hot deformation simulator Gleeble 3800, nil strength temperature of 1062°C and nil ductility temperature of 1040°C were set for CuFe2 alloy, which are unique results.
- The investigated copper alloy tested has the highest formability at approx. 1020°C. However, this is virtually unusable because high heating temperatures lead to massive grain coarsening.
- The local minimum of formability around the temperature 910°C is probably due to minor phase transformation (the formation of γ-iron).
- In the forming temperatures interval 650-950°C and strain rate 0.1-10 s^{-1} the flow stress curves were obtained and after their analysis hot deformation activation energy of 380 kJ·mol^{-1} was achieved. The value is very close to the value 389 kJ·mol^{-1} at Cu – 3.45 % Ti alloy, but due to alloying with iron much higher that at copper with purity 4N (i.e. 245 kJ·mol^{-1}).
- Throughout the deformation conditions, the two coordinates of the peak of the stress-strain curve were mathematically described with good accuracy by equations depending on Zener-Hollomon parameter. The expected phase transformation thus affected hot formability, but not peak stress values of CuFe2 alloy.
- Calculated peak strain corresponds to the start of dynamic recrystallization. Peak stress is the value appropriate for simple and fast prediction of maximum deformation resistance of the tested alloy depending on the temperature-compensated strain rate.

REFERENCES

[1] S.V. Dobatkin, J. Gubicza, D.V. Shangina, N.R. Bochvar, N.R. Tabachkova, Mater. Lett. **153**, 5-9 (2015).

[2] K. Rodak, K. Radwański, ADV. Mater. Res.-Switz. **110**, 255-265 (2016).

[3] W. He et al., T. Nonferr. Metal Soc. **19**, 93-98 (2009).

[4] A. Bachmaier, M. Kerber, D. Setman, R. Pippan, Acta. Mater. **60**, 860-871 (2012).

[5] A. Lukyanov, A. Churakova, A. Filatov, E. Levin, R. Valiev, D. Gunderov, E. Antipov, Mater. Sci. Eng. **63**, 012102 (2014).

[6] H. Cao, J.Y. Min, S.D. Wu, A.P. Xian, J.K. Shang, Mater. Sci. Eng. A. **431**, 86-91 (2006).

[7] M.Y. Alawadhi, S. Sabbaghianrad, Y. Huang, T.G. Langdon, Journal of Materials Research and Technology **256**, 2-9 (2017).

[8] K. Rodak, A. Urbańczyk-Gucwa, M.B. Jabłońska, Arch. Civ. Mech. Eng. **18**, 500-507 (2018).

[9] K. Rodak, J. Pawlicki, Mat. Char. **94**, 37-45 (2014).

[10] N. Guo, B. Song, H. Yu, R. Xin, B. Wang, T. Liu, Mat. and Des. **90**, 545-550 (2016).

[11] A.A. Hameda, L. Blaz, Scripta Mater. **37** (12), 1987-1993 (1997).

[12] S. Nagarjuna, M. Srinivas, Mater. Sci. Eng. A. **498**, 468-474 (2008).

[13] W. Gao, A. Belyakov, H. Miura, T. Sakai, Mater. Sci. Eng. A. **265**, 233-239 (1999).

[14] H. Zhang, H.-G. Zhang, D.-S. Peng, T. Nonferr. Metal Soc. **16**, 562-566 (2006).

[15] H. Okamoto, ASM International, Materials Park, OH, 131-137 (1993).

[16] Q. Chen, Z.P. Jin, Metall. Mater. Trans. A. **26A**, 418-426 (1995).

[17] K. Shubhank, Y.-B. Kang, Calphad. **45**, 127-137 (2014).

[18] I. Schindler, J. Bořuta, Arch. Metall. **39** (4), 479-491 (1994).

[19] I. Schindler, P. Kawulok, E. Hadasik, D. Kuc, J. Mater. Eng. Perform. **22** (3) 890-897, (2013).

[20] I. Schindler, R. Kawulok, H. Kulveitová, P. Kratochvíl, V. Šíma, M. Knapiński, Acta. Phys. Pol. A. **122** (3), 610-613 (2012).

[21] M.C. Sellars, W.J. McG, Tegart: Int. Metall. Rev. **17**, 1-24 (1972).

[22] I. Schindler, P. Kawulok, R. Kawulok, E. Hadasik, D. Kuc, High Temp. Mater. Proc. **32**, 149-155 (2013).

[23] C. Zener, J.H. Hollomon, J. Appl. Phys. **15**, 22-32 (1994).

[24] J. Kliber, I. Schindler, W. Kubinski, Z. Kuzminski, Steel Res. **60**, 503-508 (1989).

[25] A. Momeni, K. Dehghani, Met. Mater. Int. **16**, 843-849 (2010).

[26] A. Hameda, L. Blaz, Mater. Sci. Eng. A. **254**, 83-89 (1998).